



Development of MKIDs in the Optical and Near-Infrared Bands for SPIAKID

Hu Jie^{1,2} · Nicaise Paul¹ · Boussaha Faouzi¹ · Martin Jean-Marc¹ ·
Chaumont Christine¹ · Marret Alexine¹ · Reix Florent¹ · Firminy Josiane¹ ·
Vacelet Thibaut¹ · Pham Viet Dung² · Piat Michel² · Caffau Elisabetta¹ ·
Bonifacio Piercarlo¹

Received: 18 September 2023 / Accepted: 18 November 2023 / Published online: 13 December 2023
© The Author(s), under exclusive licence to Springer Science+Business Media, LLC, part of Springer Nature
2023

Abstract

SpectroPhotometric Imaging in Astronomy with Kinetic Inductance Detectors (SPIAKID) aims at designing, building, and deploying on the sky a spectrophotometric imager based on microwave kinetic inductance detectors (MKIDs) in the optical and near-infrared bands. MKIDs show a fast response and the ability to resolve photon energy compared to the conventional Charge-coupled Devices (CCDs). In this paper, we present the design and simulation of the MKID arrays for SPIAKID. The detectors consist of four arrays with each array of 20,000 lumped-element pixels, and each array will be read with 10 readout lines. The meander material of the resonators is trilayer TiN/Ti/TiN to have better uniformity of the critical temperature across the array. We also present the measurement result for a test array with 30×30 pixels which is a subset of the designed 2000-pixel array to verify the design and fabrication. The current measured best energy-resolving power $R = E/\Delta E$ is 2.4 at $\lambda = 405$ nm and the current medium R is around 1.7. We have also observed that the response of the TiN/Ti/TiN is much smaller than expected.

Keywords SPIAKID · MKIDs · TiN/Ti/TiN · Optical

1 Introduction

SPIAKID is an ERC-funded project that aims to open the way to a new class of wide-range, wide-field, high-efficiency, and high-angular-resolution MKIDs-based spectro-imagers via a demonstrator instrument at NTT telescope in Chile. The primary objective of the project is to perform a detailed study of the stellar populations of at least one ultra-faint dwarf galaxy [1–4] (UFD) in the local group. Other science cases are the follow-up observations of sources of gravitational waves [5] and

afterglows of gamma-ray bursts (GRBs) [6], characterization of the minor bodies of the solar system, and detection of exoplanet transits and exoplanet transit spectroscopy [7].

MKIDs show a great advantage [8, 9] over CCD cameras for their intrinsic energy resolution as well as the ability to record the arrival time of the photons. This means that for any object in the Field-of-View, one records the number of photons arrived over a given time interval and for any chosen wavelength bin, that is a spectrum, without the need to disperse the light with a prism or grating. The resolving power of such spectrum, $E/\Delta E$, is dictated by the performance of the detector. SPIAKID aims at a Field-of-View of $2' \times 2'$ in the sky. This can be achieved with four MKID arrays of 20,000 pixels each on the focal plane. Due to budgetary restrictions, we shall equip the focal plane with four arrays, but we shall read only two arrays with 10 feed lines each. Each feedline will read out 2000 pixels. The wavelength range covered by our detectors will cover the optical and near-infrared ($0.4 \mu\text{m}$ to $1.6 \mu\text{m}$).

An MKID pixel in the optical band and the near-infrared band is a superconducting resonator usually consisting of an interdigital capacitor and a meander line. Each pixel has a unique resonance frequency. All the pixels share the same meander design. Multiplexing is realized by tuning the capacitance by changing the finger length of the prototype interdigital capacitor. The resonance frequency spacing is usually on the order of 2 MHz.

The meander is usually made of superconductors with higher normal resistivity, such as TiN [10–12], TiN/Ti/TiN [13], PtSi [14], Hafnium [15], Hafnium/Indium [16] and β -Tantalum [17], which is quite challenging to keep high resistivity and high film quality. TiN/Ti/TiN for better uniformity over the wafer, relative ease of fabrication, as well as high quality.

Designing a 2000-pixel array is also not easy. First, as the capacitance becomes smaller, the length change in the finger of the interdigital capacitor becomes smaller, eventually becoming less than $1 \mu\text{m}$, which is difficult for fabrication, especially with regular uv lithography. The second is frequency collision originating from the fabrication uncertainty, especially from the size of the meander.

In this paper, we introduce the design of the MKID array for SPIAKIDs with an increasing gap in the capacitor to reduce the resonance frequency sensitivity to finger length as the resonance frequency increases.

We will also present the measurement result of an MKIDs array with 30×30 pixels, which is a subset of the designed 2000 pixels array. This resonance frequency ranges from 4–8 GHz, with a frequency spacing of about 4 MHz, which is chosen based on the limited internal quality factor of our current fabrication. The array is a key step in verifying the design and the fabrication procedure for the full array for SPIAKID.

2 MKIDs Design and Simulation

The design goal of the MKID array for SPIAKID is to design an MKID array with resonance frequencies ranging from 4 to 8 GHz with a length variation in the finger of each capacitor greater than $1 \mu\text{m}$ and a resonance spacing of about 2 MHz, making

it possible to fabricate the MKID array in ordinary lithography. Here, we gradually increase the gap between the fingers of the capacitor to reduce the capacitance sensitivity to the length of the finger. One of the designed MKIDs is shown in Fig. 1.

We select the material of the meander to be TiN/Ti/TiN [13] mainly to improve the uniformity of the film across the wafer. The film of the meander is made of TiN/Ti/TiN with a critical temperature of 1.75 K and thickness to be 10/10/10 deposited on a sapphire substrate. The resistivity of the trilayer film is about $93 \mu\Omega \cdot \text{cm}$, corresponding to kinetic inductance [18] $L_k \approx 24.5 \text{ pH}/\square$. The meander is a double-folded meander to reduce the crosstalk between the pixels [19]. The size of the meander is $36 \times 36 \mu\text{m}^2$, to accommodate the optics from the telescope, which includes a microlens set that is about 0.7 mm above the MKIDs array. The width of the meander line is $2.5 \mu\text{m}$ and the gap between the meander line is $0.5 \mu\text{m}$. The distance between the adjacent MKID pixels is $180 \mu\text{m}$, which corresponds to 0.45° on the sky based on our current optical design.

The width of the fingers in the capacitor is fixed at $1 \mu\text{m}$, while the spacing between them changes from 1 to $4.5 \mu\text{m}$ when the resonance frequency changes from 4 to 8 GHz.

We couple the resonator to the feedline with a coupling bar. The coupling quality factor of the MKIDs scales with the coupling capacitor as follows [20]

$$Q_c = \frac{2}{Z_0 L_0 C_c^2 \omega_r^3} \tag{1}$$

where Z_0 is the characteristic impedance of the feedline, L_0 is the total inductance in the resonator, C_c is the coupling capacitor to the feedline, and $\omega_r = 2\pi f_r$ is the angular frequency with f_r the resonance frequency. And C_c can be further expressed as a parallel connection of the coupling capacitor C_{cc} and the parasitic capacitor to the ground C_{c0} as

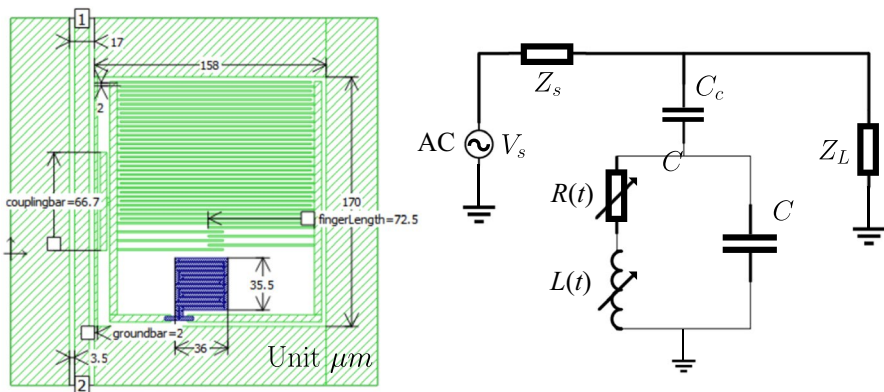


Fig. 1 One of the designed MKID pixels in the array with resonance around 6 GHz and the equivalent circuit of MKIDs

$$C_c = C_{cc} + C_{c0} \quad (2)$$

C_{cc} can be adjusted by tuning the length of the coupling bar by simulating the resonator with different lengths of the coupling bar and fitting the S_{21} of the resonator with

$$S_{21} = 1 - \frac{Q_L/Q_c}{1 + 2jQ_L\delta x} \quad (3)$$

where Q_L is the quality factor of the resonator, and $\delta x = (f - f_r)/f_r$ is the fraction of frequency shift to the resonance frequency f_r .

C_{c0} corresponds to the coupling capacitance when $C_{cc} = 0$ and tends to change with resonance frequency. To tune the Q_c to be around the desired value, which is 50,000 in our case, C_{c0} is simulated with different capacitance tuned by the finger length in the interdigital capacitor as is shown in Fig. 2A. C_{c0} tends to increase and saturate, which means that Q_c cannot be tuned further. To solve this problem, we adjust the gap width in the interdigital capacitor and the ground bar width, as shown in Fig. 1 to tune the C_{c0} . We further tune Q_c by tuning C_{cc} , which can be obtained by sweeping the coupling bar length. Once C_{c0} and C_{cc} are obtained, we interpolate the length of the coupling bar to obtain the desired Q_c which is shown in Fig. 2B. Finally, we linearly interpolate each finger to obtain the array. The change in finger length Δl is shown in Fig. 2C, and the statistics of Δl is shown in the inset of Fig. 2C, which shows that most of Δl is larger than 1 μm .

3 MKIDs Characterization

The MKIDs are measured in an adiabatic demagnetization refrigerator (ADR) at Laboratoire Astroparticule et Cosmologie (APC). The detailed measurement setup is shown in Fig. 3. The stray magnetic field is shielded by a niobium cylinder of 1.5 mm thickness and sheets of metglas 2714a around MKIDs. The MKIDs are readout by a standard homodyne mixing scheme. The input signal is generated by a signal generator attenuated 20 dB, 10 dB, and 20 dB on 4 K, 1 K, and 100 mK to reduce the thermal noise. The output signal from MKIDs is first amplified by an

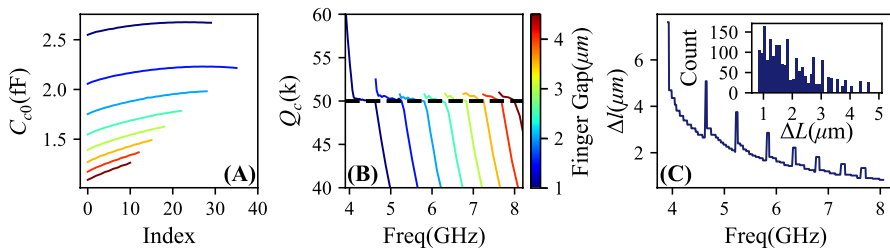


Fig. 2 **A** Simulated C_{c0} versus the number of the fingers in the capacitor that has been shorted. **B** Tuned Q_c versus the resonance frequency. **C** The change of finger length Δl versus the resonance frequency. The inset shows the statistics of Δl for the 2000-pixel array

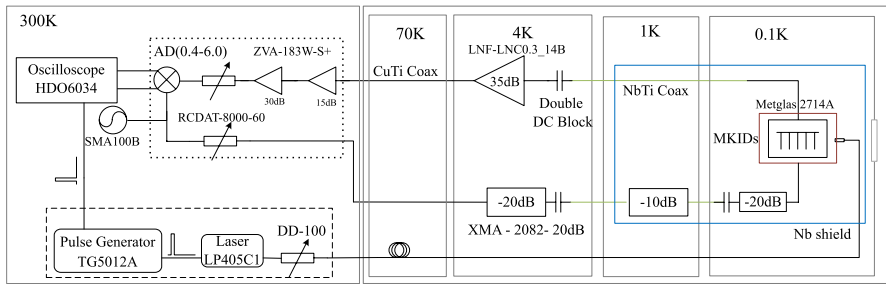


Fig. 3 Detailed measurement setup for the MKIDs in the ADR

LNA on the 4K stage and amplified further by two room-temperature amplifiers, which is the main source for the readout noise. The signal is down-converted to DC by an IQ mixer and then, sampled by an oscilloscope. Two double DC blocks are placed between the 4K and 1K stages for the operation of the heat switch in the cryostat. The MKIDs array is illuminated by an optical fiber that is placed 35 mm above the pixels. The laser is modulated by a 250 Hz pulse from the pulse generator. The output power of the laser is estimated to be a few pW outside the cryostat, attenuated by a digital step attenuator. The pulse response of the MKID is sampled by an oscilloscope (HDO6034) at 100 MHz. The S_{21} is measured by replacing the IQ mixer with a VNA. It is the same measurement setup used in our previous publications [12, 21].

The Measured MKIDs array has 30×30 pixels, which is a subset of the designed 2000-pixel array. The MKIDs were fabricated by magnetron sputtering in the clean room in Paris Observatory. The picture of the fabricated MKIDs is shown in Fig. 4B. The measured S_{21} of the array is shown in Fig. 4A. The resonance frequency starts from 4 GHz, which is in good agreement with the simulation. The resonance frequency versus the resonance index shown shows quite a good linearity, which indicates that the cross-coupling between the pixels is acceptable [19], as is shown in Fig. 4C. We have fitted Q_i with Eq. (3) in Fig. 4D and it does not show significant frequency dependence. The yield of the array is around 75%. The median internal quality factor Q_i is around 30,000, and it does not show significant frequency dependence, as is shown in Fig. 4D.

We show the single photon performance of a pixel with a resonance frequency of around 5.8 GHz in Fig. 5. The Q_i of the pixel is around 53,000. Figure 5A shows the single photon phase response of the pixel at different bath temperatures (T_{bath}) that is averaged from the full width at half maximum (FWHM) in the pulse statistics, and the inset shows the pulse maximum that increases about 50% from $T_{\text{bath}} = 150$ mK to $T_{\text{bath}} = 300$ mK. The noise spectrum at different temperatures is shown in Fig. 5B.

The pulse statistics is shown in Fig. 5C, which shows the $E/\Delta E$ to be around 2.1 @405 nm. The $1-\sigma$ width of the 1-photon peak and the 0-photon peak is 1.1 deg and 0.8 deg, respectively, which indicates the noise from readout system is not significant. It can be seen from Fig. 5D that energy-resolving power increases a bit as T_{bath} increases, which can be attributed to the increasing signal-to-noise ratio (SNR) and a

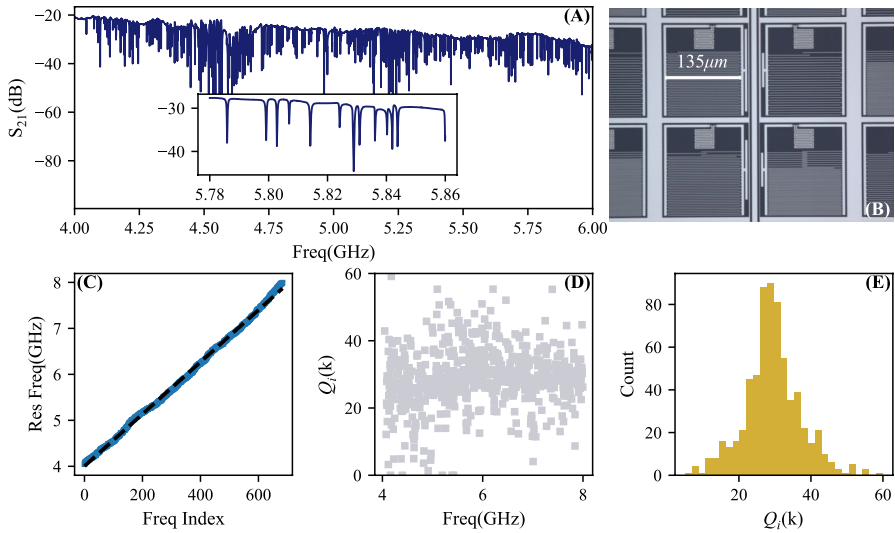


Fig. 4 Measured S_{21} for the MKIDs array and its statistics. **A** The measured S_{21} between 4–6 GHz. The inset shows the transmission between 5.78–5.86 GHz. **B** Photon of measured MKIDs chip. **C** The resonance frequency versus the resonance index. **D** The fitted Q_1 versus resonance frequency. **E** The statistics of the Q_1

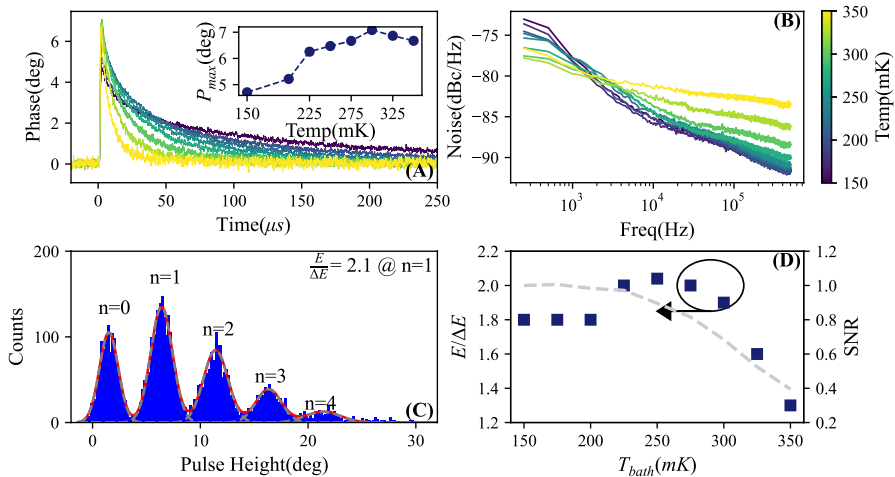


Fig. 5 **A** Averaged pulse of single photon response at 405 nm at different T_{bath} . The inset shows the maximum of the pulse response versus T_{bath} . **B** Noise spectrum measured at different T_{bath} . **C** The pulse statistics at $T_{\text{bath}} = 250$ mK. **D** Fitted energy resolution and SNR versus T_{bath}

reduction in the noise of the two-level system [22, 23], as indicated in Fig. 5C. This phenomenon has also been observed in single-layer TiN MKIDs [12], but much less significant. The $E/\Delta E$ is estimated to be around 1.2–1.4 for the same pixel based on our measurement on another array with the same design.

It should also be noted that the $E/\Delta E$ we obtained is comparable with those published results [24], considering the volume of our meander $V = 32.4 \mu\text{m}^3$. The response of the MKIDs is much smaller than what we expected. The expected response of the MKIDs is [25]

$$\phi_{qp} = \frac{\alpha S_2 Q_L}{N_0 V \Delta} \cdot \frac{\eta E}{\Delta} \quad (4)$$

where $\alpha \approx 1$ is the fraction of the kinetic inductance. $S_2 = 2.73$ is so-called the Mattis-Bardeen factor [26] with $f_0 = 5.8$ GHz, N_0 is the single spin density on the Fermi level, η is the pair-breaking efficiency, $E = 3.06$ eV is the photon energy of a 405 nm photon, and $\Delta \approx 1.76 k_B T_c$ is the energy gap of the superconductor.

If we assume $\eta = 0.6$ and $N_0 = 6.0 \times 10^{10} \text{eV}^{-1} \mu\text{m}^{-3}$, which is the value for a single-layer TiN [27], with $Q_L \approx 14,000$, the estimated $\phi_{qp} \approx 30$ deg, about 5 times higher than the value we have measured. In this case, there are two possible reasons. The first is the N_0 for the TiN/Ti/TiN film could be much higher than the single-layer TiN. The other possible reason is the pair-breaking efficiency; η is much smaller in the TiN/Ti/TiN film due to the different quasi-particle energy in different layers.

We show the statistics of the energy-resolving power of the pixels with resonance frequency between 4–6 GHz measured at 250 mK. About 330 resonators have been measured individually, about 70% of which show a single photon response. The median $E/\Delta E$ is about 1.7. We do not observe significant dependence between $E/\Delta E$ and the internal quality Q_i as well as f_r . $E/\Delta E$ tends to increase when the ratio between Q_i and Q_c increases, which is shown in Fig. 6D, which is reasonable as when $Q_i > Q_c$, the readout noise in the system tends to be suppressed as the ratio of resonance circle increases.

The main reason for this low $E/\Delta E$ is that the response of the TiN/Ti/TiN film is unexpectedly low. We would like to reduce the size to $25 \times 25 \mu\text{m}^2$ or even $15 \times 15 \mu\text{m}^2$. The second is to optimize the film quality. Currently, the T_c of the TiN/Ti/TiN is around 1.75 K. We would further optimize the film to have a $T_c = 1.2 - 1.4$ K. In this case, we hope we can get an improvement of $E/\Delta E$ with a factor of 3–4.

We stress, however, that even this low $E/\Delta E$ is sufficient for the main science goal of SPIAKID, namely the characterization of the stellar populations of Ultra Faint Dwarf galaxies (UFDs). We reached this conclusion after analyzing synthetic fluxes computed from model stellar atmospheres. The main conclusion is that stellar parameters can be extracted from a SPIAKID spectrum even if $E/\Delta E$ is as low as currently afforded by our detectors, provided it is known for any given wavelength. We used theoretical stellar fluxes, computed from one-dimensional model stellar atmospheres in hydrostatic equilibrium, computed with a resolving power $R = E/\Delta E = 200$. We used fluxes of two models with the same effective temperature and gravity, but different concentrations of elements heavier than He, and scaled the fluxes to the absolute magnitude predicted by theoretical isochrones of two different ages. Such a combination is what you can expect to find among the stellar populations of UFDs. We verified that the monochromatic magnitude difference between the two fluxes is about 0.2 magnitudes, both for the original fluxes and for

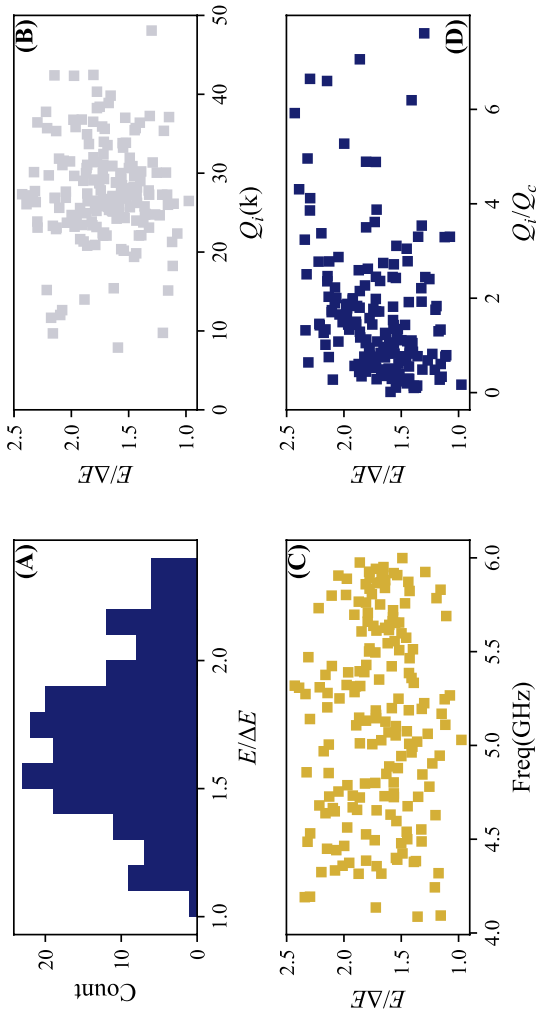


Fig. 6 A Statistics of $E/\Delta E$ for resonators from 4.3 to 6 GHz, around 330 pixels are measured. **B–D** $E/\Delta E$ versus Q_i , f_0 and Q_i/Q_c

those degraded to $R = 2.5$. Hence, it shall be, in principle, possible to derive stellar parameters from the observed SPIAKID spectra, by fitting theoretical spectra. This requires, of course, that the resolving power be known at any given wavelength. This information shall be provided by the SPIAKID calibration plan.

4 Conclusion

We have designed, fabricated, and characterized the TiN/Ti/TiN MKID array for SPIAKID. The current results show that the yield of the current design is around 75% out of 900 pixels and around 70% of measured pixels show a single photon response at 405 nm. The optimum $E/\Delta E$ is around 2.4 and the median is around 1.7. The TiN/Ti/TiN MKIDs show a similar response with bath temperature compared to the single-layer TiN MKIDs. The response of TiN/Ti/TiN is around 5 times smaller than what we expected.

Acknowledgements This work is supported by the European Research Council (ERC) through Grant 835087 (SPIAKID) and UnivEarS Labex program.

Author Contributions Dr. MRR: Conceptualization methodology, original draft preparation Dr. RNS, Dr. CAD Supervision Dr. MU-S Dr. NKS supervision, Dr. MAM supervision

Declarations

Conflict of interests The authors declare no competing interests.

References

1. B. Willman, M.R. Blanton, A.A. West, J.J. Dalcanton, D.W. Hogg, D.P. Schneider, N. Wherry, B. Yanny, J. Brinkmann. A new milky way companion: unusual globular cluster or extreme dwarf satellite? *Astron. J.* **129**(6), 2692 (2005). <https://doi.org/10.1086/430214>
2. B. Willman, J.J. Dalcanton, D. Martinez-Delgado, A.A. West, M.R. Blanton, D.W. Hogg, J.C. Barentine, H.J. Brewington, M. Harvanek, S.J. Kleinman, J. Krzesinski, D. Long, J.E.H. Neilsen, A. Nitta, S.A. Snedden, A new milky way dwarf galaxy in URSA major. *Astrophys. J.* **626**(2), 85 (2005). <https://doi.org/10.1086/431760>
3. R.J. Bouwens, G.D. Illingworth, P.A. Oesch, M. Trenti, I. Labbé, M. Franx, M. Stiavelli, C.M. Carollo, P. Dokkum, D. Magee, Lower-luminosity galaxies could reionize the universe: Very steep faint-end slopes to the UV luminosity functions at $z \approx 5-8$ from the hufd09 wfc3/ir observations. *Astrophys. J. Lett.* **752**(1), 5 (2012). <https://doi.org/10.1088/2041-8205/752/1/L5>
4. K. Bechtol, A. Drlica-Wagner, E. Balbinot, A. Pieres, J.D. Simon, B. Yanny, B. Santiago, R.H. Wechsler, J. Frieman, A.R. Walker, P. Williams, E. Rozo, E.S. Rykoff, A. Queiroz, E. Luque, A. Benoit-Lévy, D. Tucker, I. Sevilla, R.A. Gruendl, L.N.d. Costa, A.F. Neto, M.A.G. Maia, T. Abbott, S. Allam, R. Armstrong, A.H. Bauer, G.M. Bernstein, R.A. Bernstein, E. Bertin, D. Brooks, E. Buckley-Geer, D.L. Burke, A.C. Rosell, F.J. Castander, R. Covarrubias, C.B. D'Andrea, D.L. DePoy, S. Desai, H.T. Diehl, T.F. Eifler, J. Estrada, A.E. Evrard, E. Fernandez, D.A. Finley, B. Flaugher, E. Gaztanaga, D. Gerdes, L. Girardi, M. Gladders, D. Gruen, G. Gutierrez, J. Hao, K. Honscheid, B. Jain, D. James, S. Kent, R. Kron, K. Kuehn, N. Kuropatkin, O. Lahav, T.S. Li, H. Lin, M. Makler, M. March, J. Marshall, P. Martini, K.W. Merriitt, C. Miller, R. Miquel, J. Mohr, E. Neilsen, R. Nichol, B. Nord, R. Ogando, J. Peoples, D. Petravick, A.A. Plazas, A.K. Romer, A. Roodman, M. Sako, E. Sanchez, V. Scarpine, M. Schubnell, R.C. Smith, M. Soares-Santos, F. Sobreira, E. Suchyta, M.E.C. Swanson, G. Tarle, J. Thaler, D. Thomas, W. Wester, J. Zuntz, Eight

- new milky way companions discovered in first-year dark energy survey data. *Astrophys. J.* **807**(1), 50 (2015) <https://doi.org/10.1088/0004-637X/807/1/50>
5. L.S. Collaboration, C. Virgo, B.P. Abbott, R. Abbott, T.D. Abbott, M.R. Abernathy, F. Acernese, K. Ackley, C. Adams, T. Adams, P. Addesso, R.X. Adhikari, V.B. Adya, C. Affeldt, M. Agathos, K. Agatsuma, N. Aggarwal, O.D. Aguiar, L. Aiello, A. Ain, P. Ajith, B. Allen, A. Allocca, P.A. Altin, S.B. Anderson, W.G. Anderson, K. Arai, M.A. Arain, M.C. Araya, C.C. Arceneaux, J.S. Areeda, N. Arnaud, K.G. Arun, S. Ascenzi, G. Ashton, M. Ast, S.M. Aston, P. Astone, P. Aufmuth, C. Aulbert, S. Babak, P. Bacon, M.K.M. Bader, P.T. Baker, F. Baldaccini, G. Ballardin, S.W. Ballmer, J.C. Barayoga, S.E. Barclay, B.C. Barish, D. Barker, F. Barone, B. Barr, L. Barsotti, M. Barsuglia, D. Barta, J. Bartlett, M.A. Barton, I. Bartos, R. Bassiri, A. Basti, J.C. Batch, C. Baune, V. Bavigadda, M. Bazzan, B. Behnke, M. Bejger, C. Belczynski, A.S. Bell, C.J. Bell, B.K. Berger, J. Bergman, G. Bergmann, C.P.L. Berry, D. Bersanetti, A. Bertolini, J. Betzwieser, S. Bhagwat, R. Bhandare, I.A. Bilenko, G. Billingsley, J. Birch, R. Birney, O. Birnholtz, S. Biscans, A. Bisht, M. Bitossi, C. Biwer, M.A. Bizouard, J.K. Blackburn, C.D. Blair, D.G. Blair, R.M. Blair, S. Bloemen, O. Bock, T.P. Bodiya, M. Boer, G. Bogaert, C. Bogan, A. Bohe et al., Observation of gravitational waves from a binary black hole merger. *Phys. Rev. Lett.* **116**(6), 061102 (2016). <https://doi.org/10.1103/PhysRevLett.116.061102>
 6. T. Piran, The physics of gamma-ray bursts. *Rev. Mod. Phys.* **76**(4), 1143 (2005)
 7. A.M. Mandell, K. Haynes, E. Sinukoff, N. Madhusudhan, A. Burrows, D. Deming, Exoplanet transit spectroscopy using wfc3: Wasp-12 b, wasp-17 b, and wasp-19 b. *Astrophys. J.* **779**(2), 128 (2013)
 8. B.A. Mazin, S.R. Meeker, M.J. Strader, P. Szypryt, D. Marsden, J.C.V. Eyken, G.E. Duggan, A.B. Walter, G. Ulbricht, M. Johnson, Arcons: a 2024 pixel optical through near-IR cryogenic imaging spectrophotometer. *Publ. Astron. Soc. Pac.* **125**(933), 1348–1361 (2013)
 9. ...S.R. Meeker, B.A. Mazin, A.B. Walter, P. Strader, N. Fruitwala, C. Bockstiegel, P. Szypryt, G. Ulbricht, G. Coiffard, B. Bumble, G. Cancelo, T. Zmuda, K. Treptow, N. Wilcer, G. Collura, R. Dodkins, I. Lipartito, N. Zobrist, M. Bottom, J.C. Shelton, D. Mawet, J.C. Eyken, G. Vasisht, E. Serabyn, Darkness: a microwave kinetic inductance detector integral field spectrograph for high-contrast astronomy. *Publ. Astron. Soc. Pac.* **130**(988), 065001 (2018). <https://doi.org/10.1088/1538-3873/aab5e7>
 10. J. Gao, M.R. Vissers, M.O. Sandberg, F.C.S. Silva, S.W. Nam, D.P. Pappas, D.S. Wisbey, E.C. Langman, S.R. Meeker, B.A. Mazin, H.G. Leduc, J. Zmuidzinis, K.D. Irwin, A titanium-nitride near-infrared kinetic inductance photon-counting detector and its anomalous electrostatics. *Appl. Phys. Lett.* **101**(14), 142602 (2012). <https://doi.org/10.1063/1.4756916>
 11. P. Nicaise, J. Hu, J.-M. Martin, S. Beldi, C. Chaumont, P. Bonifacio, M. Piat, H. Geoffray, F. Boussaha, Investigation of optical coupling in microwave kinetic inductance detectors using superconducting reflective plates. *J. Low Temp. Phys.* **209**(5), 1242–1248 (2022). <https://doi.org/10.1007/s10909-022-02789-7>
 12. F. Boussaha, J. Hu, P. Nicaise, J.-M. Martin, C. Chaumont, P.V. Dung, J. Firminy, F. Reix, P. Bonifacio, M. Piat, H. Geoffray, Photon-counting with single stoichiometric tin layer-based optical mkids. *Appl. Phys. Lett.* (2023). <https://doi.org/10.1063/5.0147584>
 13. M.R. Vissers, J. Gao, M. Sandberg, S.M. Duff, D.S. Wisbey, K.D. Irwin, D.P. Pappas, Proximity-coupled TI/TIN multilayers for use in kinetic inductance detectors. *Appl. Phys. Lett.* (2013). <https://doi.org/10.1063/1.4804286>
 14. P. Szypryt, S.R. Meeker, G. Coiffard, N. Fruitwala, B. Bumble, G. Ulbricht, A.B. Walter, M. Daal, C. Bockstiegel, G. Collura, N. Zobrist, I. Lipartito, B.A. Mazin, Large-format platinum silicide microwave kinetic inductance detectors for optical to near-IR astronomy. *Opt. Express* **25**(21), 25894–25909 (2017). <https://doi.org/10.1364/OE.25.025894>
 15. N. Zobrist, G. Coiffard, B. Bumble, N. Swimmer, S. Steiger, M. Daal, G. Collura, A.B. Walter, C. Bockstiegel, N. Fruitwala, I. Lipartito, B.A. Mazin, Design and performance of hafnium optical and near-IR kinetic inductance detectors. *Appl. Phys. Lett.* (2019). <https://doi.org/10.1063/1.5127768>
 16. N. Zobrist, W.H. Clay, G. Coiffard, M. Daal, N. Swimmer, P. Day, B.A. Mazin, Membraneless phonon trapping and resolution enhancement in optical microwave kinetic inductance detectors. *Phys. Rev. Lett.* **129**(1), 017701 (2022). <https://doi.org/10.1103/PhysRevLett.129.017701>
 17. K. Kouwenhoven, D. Fan, E. Biancalani, S.A.H. Rooij, T. Karim, C.S. Smith, V. Murugesan, D.J. Thoen, J.J.A. Baselmans, P.J. Visser, Resolving power of visible-to-near-infrared hybrid

- β -Ta/Nb-Ti-N kinetic inductance detectors. *Phys. Rev. Appl.* **19**(3), 034007 (2023). <https://doi.org/10.1103/PhysRevApplied.19.034007>
18. J.S. Gao, The physics of superconducting microwave resonators. PhD thesis, Caltech (2008)
 19. O. Noroozian, P.K. Day, B.H. Eom, H.G. Leduc, J. Zmuidzinas, Crosstalk reduction for superconducting microwave resonator arrays. *IEEE Trans. Microw. Theory Tech.* **60**(5), 1235–1243 (2012). <https://doi.org/10.1109/tmtt.2012.2187538>
 20. O. Noroozian, Superconducting Microwave Resonator Arrays for Submillimeter/Far-Infrared Imaging. PhD thesis, Caltech (2012)
 21. J. Hu, M. Salatino, A. Traini, C. Chaumont, F. Boussaha, C. Goupil, M. Piat, Proximity-coupled Al/Au bilayer kinetic inductance detectors. *J. Low Temp. Phys.* **199**(1), 355–361 (2020). <https://doi.org/10.1007/s10909-019-02313-4>
 22. J. Gao, M. Daal, A. Vayonakis, S. Kumar, J. Zmuidzinas, B. Sadoulet, B.A. Mazin, P.K. Day, H.G. Leduc, Experimental evidence for a surface distribution of two-level systems in superconducting lithographed microwave resonators. *Appl. Phys. Lett.* **92**(15), 152505 (2008). <https://doi.org/10.1063/1.2906373>
 23. J. Hu, F. Boussaha, J.-M. Martin, P. Nicaise, C. Chaumont, S. Beldi, M. Piat, P. Bonifacio, Large inverse transient phase response of titanium-nitride-based microwave kinetic inductance detectors. *Appl. Phys. Lett.* (2021). <https://doi.org/10.1063/5.0074103>
 24. W. Guo, X. Liu, Y. Wang, Q. Wei, L.F. Wei, J. Hubmayr, J. Fowler, J. Ullom, L. Vale, M.R. Vissers, J. Gao, Counting near infrared photons with microwave kinetic inductance detectors. *Appl. Phys. Lett.* **110**(21), 212601 (2017). <https://doi.org/10.1063/1.4984134>
 25. M. Martinez, L. Cardani, N. Casali, A. Cruciani, G. Pettinari, M. Vignati, Measurements and simulations of athermal phonon transmission from silicon absorbers to aluminum sensors. *Phys. Rev. Appl.* (2019). <https://doi.org/10.1103/PhysRevApplied.11.064025>
 26. J. Zmuidzinas, Superconducting microresonators: physics and applications. *Ann. Rev. Condens. Matter Phys.* **3**(1), 169–214 (2012). <https://doi.org/10.1146/annurev-conmatphys-020911-125022>
 27. A. Kardakova, M. Finkel, D. Morozov, V. Kovalyuk, P. An, C. Dunscombe, M. Tarkhov, P. Mauskopf, T.M. Klapwijk, G. Goltsman, The electron–phonon relaxation time in thin superconducting titanium nitride films. *Appl. Phys. Lett.* (2013). <https://doi.org/10.1063/1.4851235>

Publisher's Note Springer Nature remains neutral with regard to jurisdictional claims in published maps and institutional affiliations.

Springer Nature or its licensor (e.g. a society or other partner) holds exclusive rights to this article under a publishing agreement with the author(s) or other rightsholder(s); author self-archiving of the accepted manuscript version of this article is solely governed by the terms of such publishing agreement and applicable law.

Authors and Affiliations

Hu Jie^{1,2} · Nicaise Paul¹ · Boussaha Faouzi¹ · Martin Jean-Marc¹ ·
Chaumont Christine¹ · Marret Alexine¹ · Reix Florent¹ · Firminy Josiane¹ ·
Vacelet Thibaut¹ · Pham Viet Dung² · Piat Michel² · Caffau Elisabetta¹ ·
Bonifacio Piercarlo¹

✉ Hu Jie
jie.hu@obspm.fr

Nicaise Paul
paul.nicaise@obspm.fr

Boussaha Faouzi
faouzi.boussaha@obspm.fr

Martin Jean-Marc
jeanmarc@caltech.edu

Chaumont Christine
christine.chaumont@obspm.fr

Marret Alexine
alexine.marret@obspm.fr

Reix Florent
Florent.reix@obspm.fr

Firminy Josiane
josiane.firminy@obspm.fr

Vacelet Thibaut
thibaut.vacelet@obspm.fr

Pham Viet Dung
phamvd@apc.in2p3.fr

Piat Michel
piat@apc.in2p3.fr

Caffau Elisabetta
Elisabetta.caffau@obspm.fr

Bonifacio Piercarlo
piercarlo.bonifacio@obspm.fr

¹ GEPI, Observatoire de Paris, PSL Université, CNRS, 77 Avenue Denfert-Rochereau, 75014 Paris, France

² Astroparticule et Cosmologie, Université de Paris, CNRS, 10, Rue Alice Domon et Léonie Duquet, 75013 Paris, France